Laser scattering by Transcranial rat brain illumination

Marcelo V. P. Sousa[*a], Renato Prates[b], Ilka T Kato[b], Caetano P. Sabino[b], Luis C. Suzuki[b], Martha S. Ribeiro[b], Elisabeth M. Yoshimura[a].
[a]Institute of Physics, University of São Paulo, São Paulo, Brazil; [b]Center for Laser and Applications, IPEN-CNEN/SP, Brazil

ABSTRACT

Due to the great number of applications of Low-Level-Laser-Therapy (LLLT) in Central Nervous System (CNS), the study of light penetration through skull and distribution in the brain becomes extremely important. The aim is to analyze the possibility of precise illumination of deep regions of the rat brain, measure the penetration and distribution of red (λ = 660 nm) and Near Infra-Red (NIR) (λ = 808 nm) diode laser light and compare optical properties of brain structures. The head of the animal (*Rattus Novergicus*) was epilated and divided by a sagittal cut, 2.3 mm away from mid plane. This section of rat's head was illuminated with red and NIR lasers in points above three anatomical structures: hippocampus, cerebellum and frontal cortex. A high resolution camera, perpendicularly positioned, was used to obtain images of the brain structures. Profiles of scattered intensities in the laser direction were obtained from the images. There is a peak in the scattered light profile corresponding to the skin layer. The bone layer gives rise to a valley in the profile indicating low scattering coefficient, or frontal scattering. Another peak in the region related to the brain is an indication of high scattering coefficient (μ_s) for this tissue. This work corroborates the use of transcranial LLLT in studies with rats which are subjected to models of CNS diseases. The outcomes of this study point to the possibility of transcranial LLLT in humans for a large number of diseases.

Keywords: LLLT dosimetry, rat brain illumination, Nervous System, Biophotonics, Near Infra-Red laser, Transcranial Illumination, Hippocampus, Neurology, LLLT animal model, Neurophotonics.

1. INTRODUCTION

Just few years after Theodore Maiman [1] developed the first laser in 1960, it was used by Mester [2] to promote wound healing, and this is probably the first Low Level Laser Therapy (LLLT). The mechanisms of LLLT is based in photon absorption by molecules, it was first explained by Karu [3]. Laser illumination promotes DNA and RNA synthesis [4], lead protein production and increase mitochondrial production of ATP accelerating cell metabolism [5]. Nowadays LLLT is being used in branches of medicine that require reduction of inflammation, pain relief, healing, tissue regeneration or prevention of tissue death [6].

Recently remarkable results have been found in Neurology, using Transcranial LLLT, a noninvasive treatment for serious brain diseases or injuries. Transcranial LLLT improves motor recovery after strokes in rats [7] and in humans [8]; reduces significantly the recovery time in Traumatic Brain Injury (TBI) [9] with little evidence of side effects [10]. Encouraging results were obtainded for some degenerative CNS diseases as familial amyotrophic lateral sclerosis [11], Parkinson disease [12], Alzheimer disease [13] with this technique. Additionally, single neuron light stimulation [14] is connected to pain relief.

Light crossing the interior of biological tissue interacts, basically, in two ways: absorption and scattering [15]. The absorption occurs when a photon interacts with an atom or molecule and the entire energy of the photon is transferred to the atom or molecule. Absorption is quantified by the absorption coefficient (μ_a), which is related to the probability of this interaction in a unit of length. The scattering interactions can change both direction and energy of photons (inelastic), or only the direction (elastic scattering). Visible and near IR light interacting with biological tissue give rise mainly to elastic scattering. The scattering depends on size, shape and refraction index of the scattering center and on the wavelength of the incident light. To quantify elastic scattering two parameters are necessary: the scattering coefficient (μ_s), which express the probability that scattering occurs, and the anisotropy factor (g), which is defined as the average cosine of the scattering angle. The total attenuation coefficient is $\mu_t = \mu_a + \mu_s$.

Knowledge of the penetration and distribution of light inside biological tissues is a hard problem because absorption and scattering depend on wavelength, tissue biochemistry and anatomy [16]. Numerical methods as Monte Carlo simulation [17] can be used to calculate light distribution inside tissues. Due to inhomogeneity of biological tissues, transport theory, a heuristic approach based on energy conservation, is more useful than Maxwell equations to analyze light distribution inside biological medium [16]. The amount of photons in a position $\vec{r}$ propagating in a given direction $\vec{s}$ is described by the radiative transport equation:

Biophotonics: Photonic Solutions for Better Health Care III, edited by Jürgen Popp, Wolfgang Drexler, Valery V. Tuchin, Dennis L. Matthews, Proc. of SPIE Vol. 8427, 842728

$$\frac{dL(\vec{r},\vec{s})}{ds} = -\mu_t L(\vec{r},\vec{s}) + \mu_s \int_{4\pi} p(\vec{s},\vec{s'})\, L(\vec{r},\vec{s'}) d\Omega, \quad (1)$$

where $L(\vec{r},\vec{s})$ is the radiance and $p(\vec{s},\vec{s'})$ is the phase function that describes the angular distribution for a single scattering event.

Here we present an experimental study that was carried out to determine light penetration and distribution inside the animal heads, during transcranial rat brain illumination. The imaging technique allows us to determine light fluence inside skin, bone, brain and to obtain a relative attenuation coefficient for each tissue [18].

2. MATERIAL AND METHODS

Two diode laser sources were used in this experiment (λ = 808 nm e λ = 660 nm), main characteristics of these sources are presented in table 1. A neutral variable filter was used to regulate light intensity and a high resolution camera (14.7 Mega pixels) captured photons scattered from the sample. The camera lenses were adjusted to focus in the surface of the sample. As the sensitivity of the camera is very low for NIR, exposure time was 4.0 s for NIR light and 10 ms for red light. Short period illumination generated speckle patterns to red illuminations.

Table 1: Characteristics of laser sources.

Source	λ (nm)	Power (mW)	Angular aperture of the beam (°)	Spot size (mm)
Red	660	30	30	1.40
NIR	808	30	30	1.40

Adult rats (*Rattus Novergicus*) were anesthetized, decapitated and their heads were shaved. The heads were surgically sectioned by a sagittal cut, 2.3 mm away from mid plane. This section of rat's head was illuminated with red and NIR lasers in points above three anatomical structures: hippocampus, cerebellum and frontal cortex (positions relative to the bregma were: - 3.3 mm, - 6.0 mm, + 2.5 mm, respectively). The illumination spots were 2.0 mm away from the plane surface of the sagittal cut. A coronal cut of the heads (- 3.3 mm from bregma) was also made to allow the visualization of hippocampus through another direction. Illumination spots to coronal sever were 2.3 mm away from the mid plane and 2.0 away from visualized surface (figure 1).

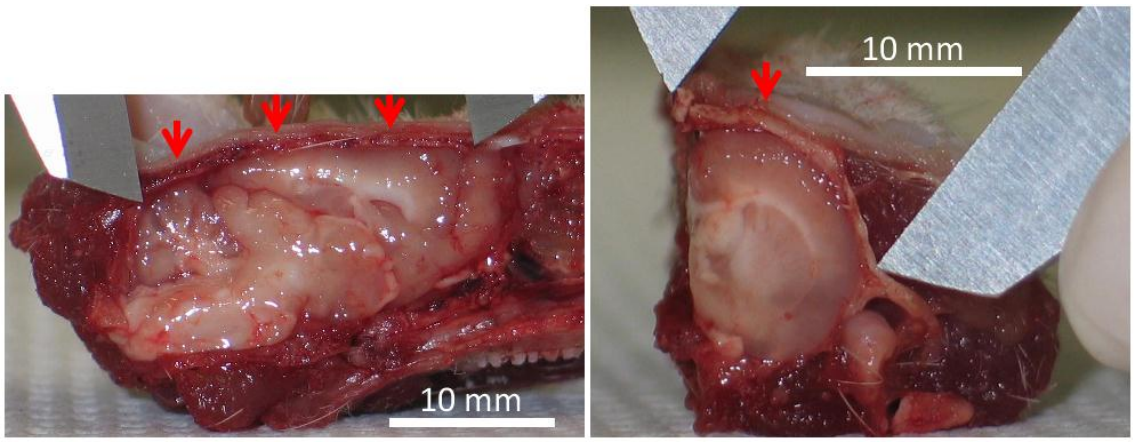

Figure 1: Sagittal (left) and coronal (right) cuts of a rat head. The arrows indicate illumination spots (left: hippocampus, cerebellum and frontal cortex, and right: hippocampus).

2.1 Experimental method

The light scattered by each sample passed through the filter and was captured by the high resolution camera which was positioned perpendicularly to the laser beam (figure 2). The images produced by the scattered light and captured by the camera were analyzed with the software ImageJ 1.44. Intensity profiles, in laser beam direction (*z*), provide information about tissue optical properties. Profiles of scattered intensities in the laser direction were obtained from the images which are in 8-bits format, so they have 256 gray-levels (gl).

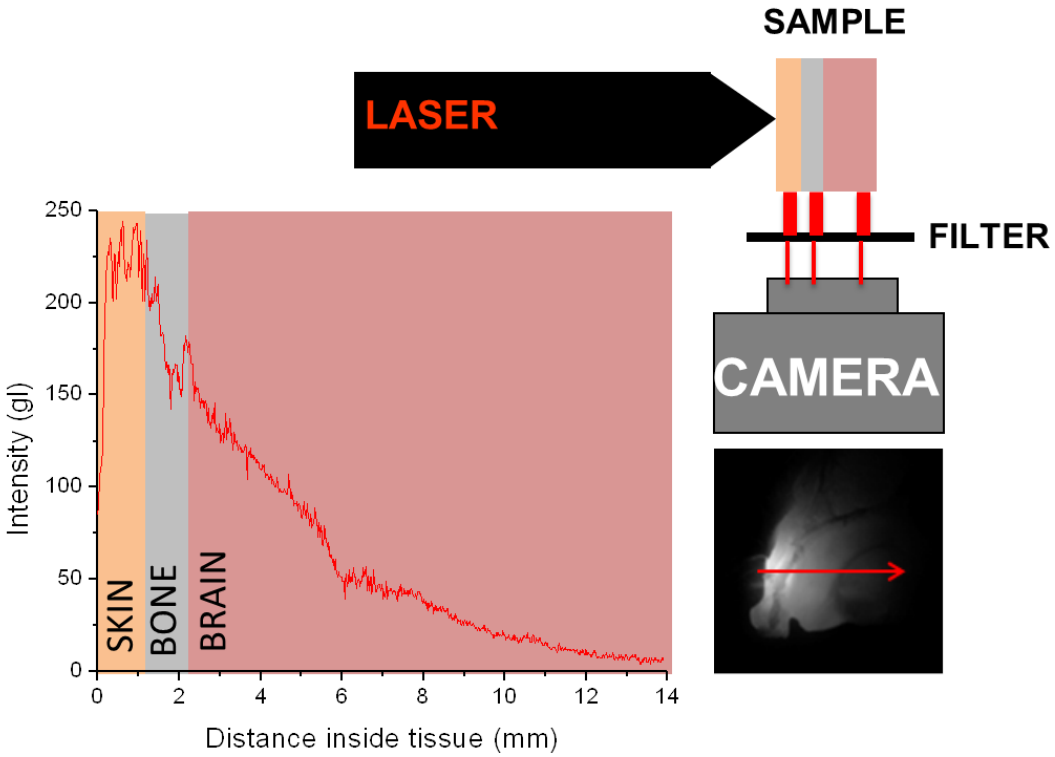

Figure 2: Set up of the experiment, laser illuminates the sample and scattered light is captured by the camera. Arrow in the image indicates where the light intensity (measured in gray levels in the image – gl) profile shown in the graph was measured.

2.2 Analyzing the images

Light scattered at 90° by homogeneous samples shows an intensity profile with a steep growth near the illumination spot, followed by an exponential attenuation [19]. In this experiment we illuminated three different tissues: skin, cranial bone and brain. The profiles of scattered intensities in the laser direction show peaks after each tissue boundary and, far from the edges, they show an approximately exponential attenuation. The peaks are higher for tissues that scatter more light. This way, one can scale tissue scattering coefficients with the corresponding peak intensity. We calculated the exponential coefficients for brain tissue profiles.

Brain is a complex organ with different kinds of neurons and glia. Shape, density, myelination and biochemical composition of cells exert major influence on brain tissue optical parameters. Profiles helped us to identify different brain regions allowing us to make a map of brain tissue optical parameters. It is possible to extract iso-intensity curves from the images.

3. RESULTS AND DISCUSSION

The images shown in figure 3 were produced with scattered light: NIR (λ = 808 nm) at top, red (λ = 660 nm) at bottom; and from left to right: hippocampus, cerebellum, frontal cortex and coronal view of hippocampus. Comparing images produced with NIR and red light one is able to notice that NIR penetrates deeper than red light. It suggests that NIR is more indicated to LLLT in inner parts of the brain. The tissue boundaries and the differences of attenuation inside the brain are qualitatively clear in the pictures.

Analyzing intensities profiles of NIR-light images (figure 4) one can see that there is a peak in the scattered light profile corresponding to the skin layer. The peak width depends on the thickness of skin in that point, and indicates the high scattering coefficient of skin. The bone layer gives rise to a valley in the profile indicating low scattering coefficient, or frontal scattering. The valley width is proportional to cranial thickness in that point. The following peak in the region related to the brain is an indication of high scattering coefficient (μ_s) for this tissue. Profiles of red-light (figure 5) images are similar to NIR-light ones but attenuation is larger and speckle pattern of the images diminishes the smoothness of the profiles.

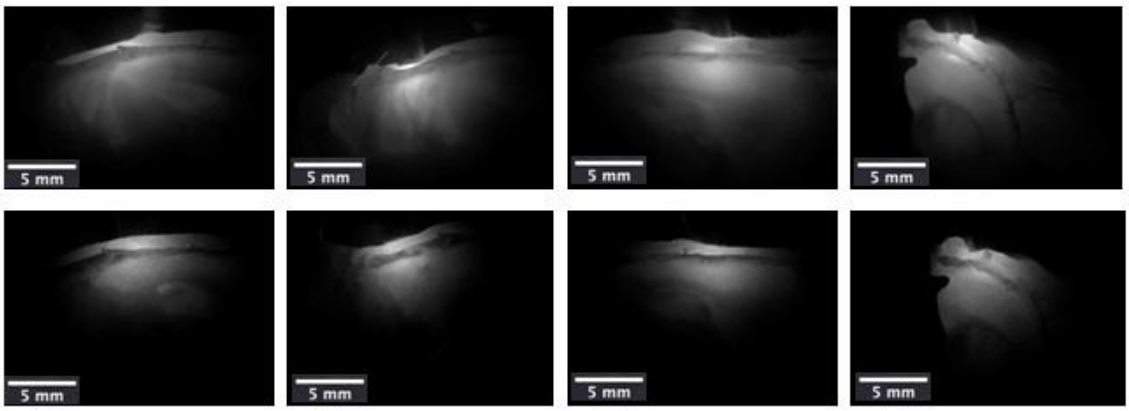

Figure 3: Images of transcranial illumination. Images of NIR illumination are at the top and red illumination ones are at the bottom. From left to right: hippocampus, cerebellum, frontal cortex and coronal view of hippocampus.

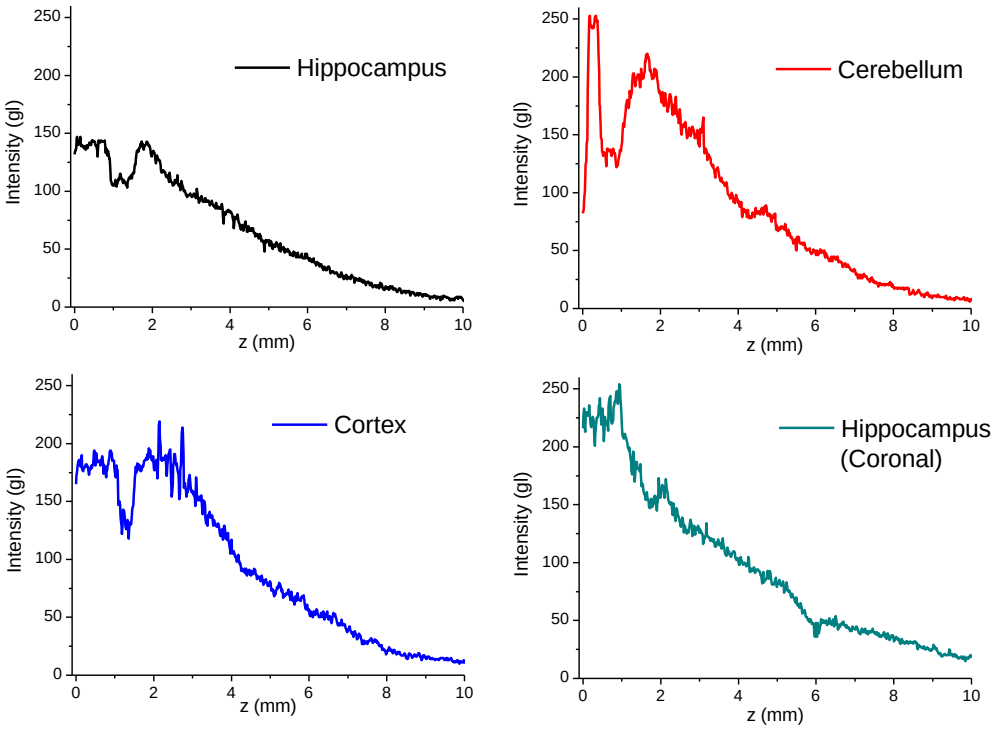

Figure 4: Profiles of transcranial illumination in different point. NIR (λ = 808 nm) illumination.

Far from the entrance, light attenuation is approximately exponential:

$$I(z) = I_0 e^{-\mu_t z} \tag{2}$$

So, we can obtain μ_t by:

$$\mu_t = -\frac{\ln\left(\frac{I(z)}{I_0}\right)}{z} \tag{3}$$

The light captured by the camera, at *z*, is proportional to *I*(*z*).. Each region of the brain has specific optical properties, so it changes the exponential coefficient. Comparing profiles, far from boundaries (*z* from 3.5 to 10.0 mm), we found differences in exponential coefficient for each point (hippocampus, cerebellum and frontal cortex), in sagittal cuts (figure 6); and differences for each direction (sagittal and coronal) in hippocampus (figure 7). As μ_t are proportional to exponential coefficients, we normalized them, making the highest value to be equal to 1, in arbitrary units (a.u.). Almost all values of μ_t, are independent, showing the strong dependence of μ_t with brain's region. Nevertheless, μ_t are statistically

equal (*) to cerebellum and hippocampus (coronal). Comparing μ_t, to red and NIR illuminations, we can see clearly that red light is more attenuated to all these brain's sub-structures (figure 8).

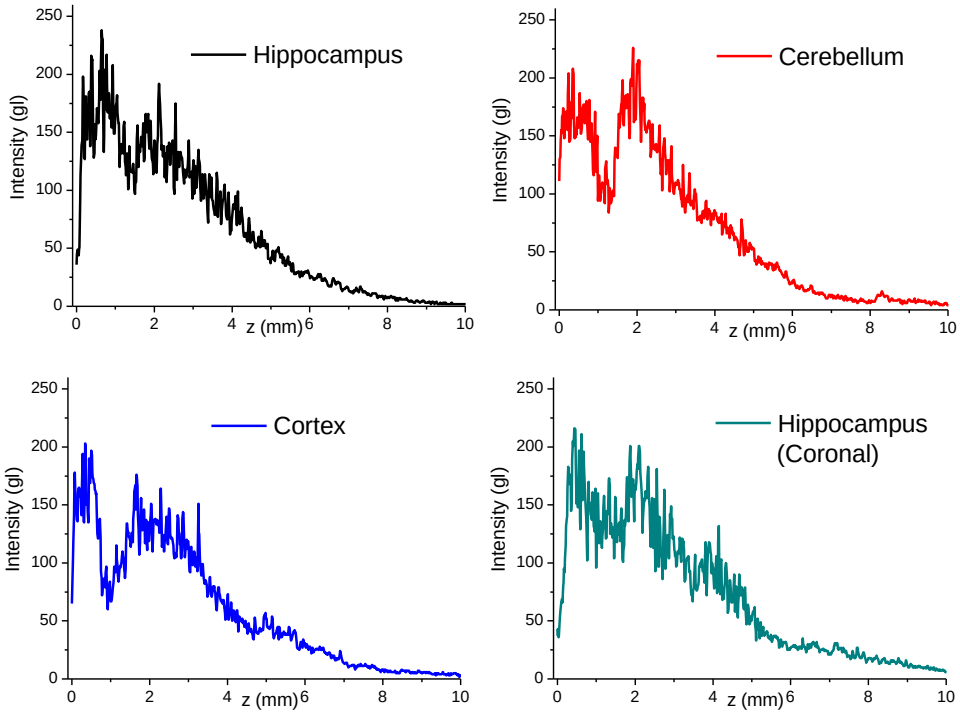

Figure 5: Profiles of transcranial illumination in different spots. Red (λ = 660 nm) illumination.

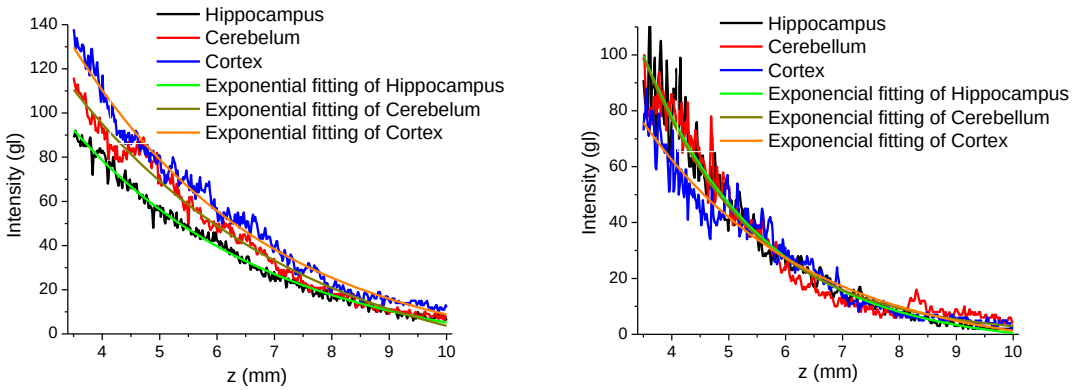

Figure 6: Exponential fitting of profiles far from boundaries to obtain μ_t (sagittal cuts).

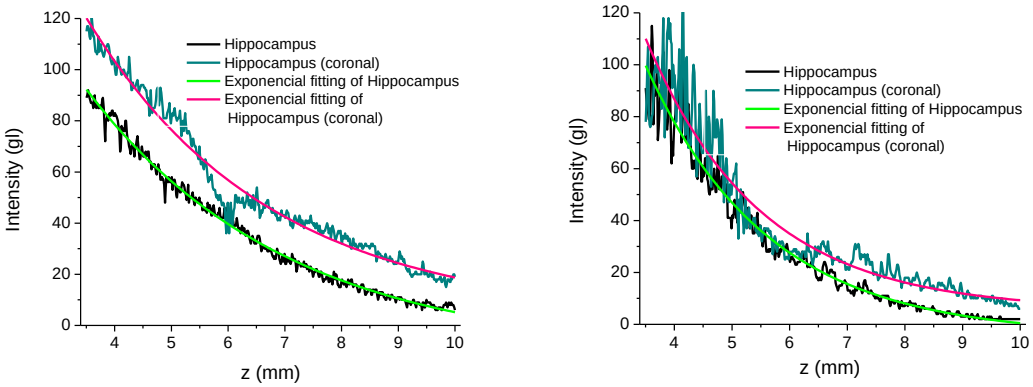

Figure 7: Exponential fitting of profiles far from boundaries to obtain μ_t (hippocampus).

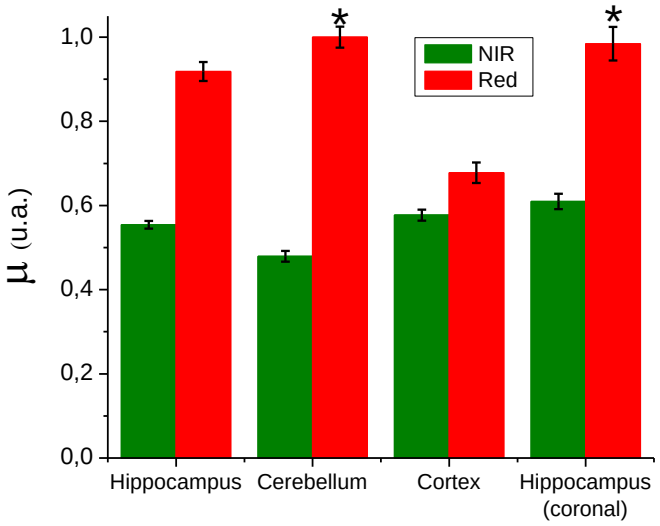

Figure 8: Normalized μ_t for red and NIR wavelengths in different brain spots. Attenuation is statistically the equal (*) for red light in cerebellum and hippocampus (coronal),

4. CONCLUSIONS

NIR penetrates deeper in a transcranial illumination, skull is not a major attenuator tissue, different parts of brain have different attenuation coefficient; these are useful information to trancranial LLLT. Analyze intensity profiles of images from tissues is a simple and powerful method to study quantitatively and qualitatively optical properties.

ACKNOWLEGEMENTS

The authors thank to CNPq and SPIE Student Chapter for financial support (Officer Travel Grant).

REFERENCES

[1] Perkowitz, “From ray-gun to Blu-ray”, Physics World, 23 (5): 16-20, (2010).
[2] Mester E., Spiry T., et al, “Effect of laser rays on wound healing”, Am J Surg,122:532-535, (1971).
[3] Karu T., “Primary and secondary mechanisms of action of visible to near-IR radiation on cells”. Journal Photochem Photobiol B; 49:1-17, (1999).
[4] Kam T., Kalendo G., Lethokov V., “Biostimulation of HeLa cells by low-intensity visible light II. Stimulation of DNA and RNA synthesis in a wide spectral range”, Nuevo Cimento;309-318, (1984).
[5] Baxter G. D. “Therapeutic Lasers: Theory and Practice”, London, England: Churchill Livingstone; 89-138, (1984).
[6] J. T. Hashmi, et al., “Role of Low-Level Laser Therapy in Neurorehabilitation”, Phys. Med. & Rehab. 2, pp. S292–S305, (2010).

[7] Lampl Y. “Laser treatment for stroke”, Expert Rev Neurother; 7:961-965, (2007).
[8] Lampl Y., Zivin J. A., Fisher M., et al. “Infrared laser therapy for ischemic stroke: a new treatment strategy: results of the NeuroThera Effectiveness and Safety Trial-1 (NEST-1)”, Stroke; 38:1843-1849, (2007).
[9] Oron A., Oron U., Streeter J., et al. “Low-level laser therapy applied transcranially to mice following traumatic brain injury significantly reduces longterm neurological deficits”, J Neurotrauma; 24:651-656, (2007).
[10] Hamblin M., Huang Y. Y., et al., “Low-level light therapy aids traumatic brain injury”, SPIE Newroonm. (2011)
[11] Moges H., Vasconcelos O. M., Campbell W. W., et al. “Light therapy and supplementary riboflavin in the SOD1 transgenic mouse model of familial amyotrophic lateral sclerosis (FALS)”, Lasers Surg Med; 41:52-59, (2009).
[12] Trimmer P. A., Schwartz K. M., Borland M. K., et al. “Reduced axonal transport in Parkinson’s disease cybrid neurites is restored by light therapy”, Mol Neurodegener; 4:26, (2009).
[13] Zhang L., Xing D., Zhu D., et al. “Low-power laser irradiation inhibiting Abeta25-35-induced PC12 cell apoptosis via PKC activation”, Cell Physiol Biochem; 22:215-222, (2008).
[14] Hirase H., Yuste R., et al. “Multiphoton Stimulation of Neurons”, Inc. J Neurobiol 51: 237–247, (2002).
[15] Sousa M. V. P., Yoshimura E. M., et al. “Phantoms of fingers with various tones of skin for LLLT dosimetry”, Proceedings of SPIE 7906, 79060U (2011)
[16] Cheong W., Prahl S. A., Welch A. J., “A review of the optical properties of the biological tissues”, Jornal of Quantum Eletronics, 26 (12): 2166 - 2185, (1990).
[17] Ramos A. Sousa M. V. P. Yoshimura E. M., et al, “Monte Carlo simulations combined with experimental measurements: a new possibility of study of the light distribution in fat emulsions.” proceedings SPIE 7567, 756709 (2010).
[18] Silva D.F.T, Ribeiro M.S. “Light attenuation in rat skin following low level laser therapy on burn healing process”, Proceedings SPIE 7715, 77151O-1 (2010).
[19] SOUSA, M. V. P., Ramos A. L. O, Magalhães A. C., Saito M. T., Yoshimura E. M., Light distribution in phantoms, Brazilian Journal of Medical Physics, 2011. v.5. p.70.

*contact: marcelovictor@usp.br